12. Thomas, R. K. & Boyd, M. G. A comparison of *Cebus albifrons* and *Samiri sciureus* on oddity performance. *Anim. Learn. Behav.* **1,** 151–153 (1973).
13. Herman, L. M. & Gordon, J. A. Auditory delayed matching in the bottlenose dolphin. *J. Exp. Anal. Behav.* **21,** 19–26 (1974).
14. Zentall, T. R. & Hogan, D. E. Same/different concept learning in the pigeon: the effect of negative instances and prior adaptation to transfer stimuli. *J. Exp. Anal. Behav.* **30,** 177–186 (1978).
15. Holmes, P. W. Transfer of matching performance in pigeons. *J. Exp. Anal. Behav.* **31,** 103–114 (1979).
16. Lombardi, C. M., Fachinelli, C. G. & Delius, J. D. Oddity of visual patterns conceptualized by pigeons. *Anim. Learn. Behav.* 12, 2–6 (1984).
17. D'Amato, M. R., Salmon, D. P. & Colombo, M. Extent and limits of the matching concept in monkeys (*Cebus apella*). *J. Exp. Psychol. Anim. Behav. Proc.* **11,** 35–51 (1985).
18. Wilson, B., Mackintosh, N. J. & Boakes, R. A. Transfer of relational rules in matching and oddity learning by pigeons and corvids. *Quart. J. Exp. Psychol.* **37B,** 313–332 (1985).
19. Oden, D. L., Premack, D. & Thompson, R. K. R. Spontaneous transfer of matching by infant chimpanzees. *J. Exp. Psychol. Anim. Behav. Proc.* **14,** 140–145 (1988).
20. Wright, A. A., Santiago, H. C., Urcuioli, P. J. & Sands, S. F. in *Quantitative Analyses Of Behavior: Discrimination Processes* Vol. IV (eds Commons, M. L., Herrnstein, R. J. & Wagner, A. R.) 295–317 (Ballinger, Cambridge MA, 1984).
21. Davey, G. *Ecological Learning Theory* (Routledge, London, 1989).
22. Menzel, R. & Giurfa, M. Cognitive architecture of a mini-brain: the honeybee. *Trends Cognit. Sci.* **5,** 62–71 (2001).
23. Hammer, M. The neural basis of associative reward learning in honeybees. *Trends Neurosci.* **20,** 245–252 (1997).

Acknowledgements

We thank C. Bönisch and C. Wiley for help with experiments 5 and 6. M.G., A.J. and R.M. were supported by the Special Programme SFB 515 of the Deutsche Forschungsgemeinschaft. M.G. was also supported by a grant from the Deutsche Forschungsgemeinschaft. S.W.Z. and M.S. were supported partly by a grant from the Human Frontiers in Science Program and from the US Defence Advanced Research Projects Agency and the Office of Naval Research. The two laboratories contributed equally to the work.

Correspondence and requests for materials should be addressed to M.G. (e-mail: giurfa@cict.fr) or S.W.Z. (e-mail: swzhang@rsbs.anu.edu.au).

Chromatic sensitivity of ganglion cells in the peripheral primate retina

Paul R. Martin*, Barry B. Lee†‡, Andrew J. R. White*, Samuel G. Solomon* & Lukas Rüttiger†

* *Department of Physiology and Institute for Biomedical Research, University of Sydney, NSW 2006, Australia*
† *Neurobiology group, Max-Planck-Institute for Biophysical Chemistry, D37077 Göttingen, Germany*
‡ *State College of Optometry, SUNY, New York, New York 10036-8003, USA*

Visual abilities change over the visual field. For example, our ability to detect movement is better in peripheral vision than in foveal vision, but colour discrimination is markedly worse[1,2]. The deterioration of colour vision has been attributed to reduced colour specificity in cells of the midget, parvocellular (PC) visual pathway in the peripheral retina[3–5]. We have measured the colour specificity (red–green chromatic modulation sensitivity) of PC cells at eccentricities between 20 and 50 degrees in the macaque retina. Here we show that most peripheral PC cells have red–green modulation sensitivity close to that of foveal PC cells. This result is incompatible with the view that PC pathway cells in peripheral retina make indiscriminate connections ('random wiring') with retinal circuits devoted to different spectral types of cone photoreceptors[4,6,7]. We show that selective cone connections can be maintained by dendritic field anisotropy, consistent with the morphology of PC cell dendritic fields in peripheral retina[8,9]. Our results also imply that postretinal mechanisms contribute to the psychophysically demonstrated deterioration of colour discrimination in the peripheral visual field.

In primates, ganglion cells of the midget, parvocellular pathway (PC cells) are proposed to be the origin of the red–green channel for colour vision[3,10–12]. Most foveal PC cells show chromatic opponent responses: they are excited by some wavelengths in the visible spectrum and inhibited by others. Chromatic opponency of PC cells in the fovea is thought to depend on the fact that they derive input to the receptive field centre from an individual middle (M) or long (L) wavelength-sensitive cone through a midget bipolar cell[4,6,13]. In peripheral retina, the receptive field centres (and dendritic fields) of PC cells are much larger than those in the fovea, and encompass the area of 20–40 M and L cones[8,9] (Fig. 1a, b). The M and L cones show little or no spatial clustering[14,15]; therefore, if the peripheral PC cells draw their receptive field centre indiscriminately from the cones in their dendritic field, they will receive mixed spectral input, and show reduced red–green chromatic sensitivity in comparison to their foveal counterparts. Mixed spectral input to PC cells has been proposed as the basis for the decline in chromatic sensitivity in peripheral vision (the 'random wiring' hypothesis)[3–5].

To test directly the random wiring hypothesis, we made extracellular single-cell recordings from the intact eye of anaesthetized macaque monkeys using standard techniques[12,16]. Recording sites were concentrated in peripheral retina between 20 and 50 degrees eccentricity (Fig. 1c). Cells were classified by receptive field tests[11,17,18], including measurement of receptive field dimensions, and measurement of contrast sensitivity using luminance-matched red and green light-emitting diodes (LEDs; Fig. 1d)[12]. Unexpectedly, when tested with hand-held stimuli, most peripheral PC cells (34/53, 64%) displayed overt red–green opponent responses. Quantitative analysis of 35 peripheral PC cells revealed 28 (80%) in which response amplitude to isoluminant red–green exchange exceeded the response amplitude for luminance change (produced by in-phase modulation of the red and green LEDs). This is an unambiguous sign of cone opponency[16]. Average red–green modulation sensitivity of opponent PC cells with receptive fields above 30 degrees eccentricity (0.836 ± 0.53 (mean $\pm$ s.d.), $n = 11$; Fig. 2a, b) was not significantly different from the average value for a sample of 18 foveal cells (1.207 ± 0.46)[12]. As expected[1,2], however, the average sensitivity for three human observers, viewing the same

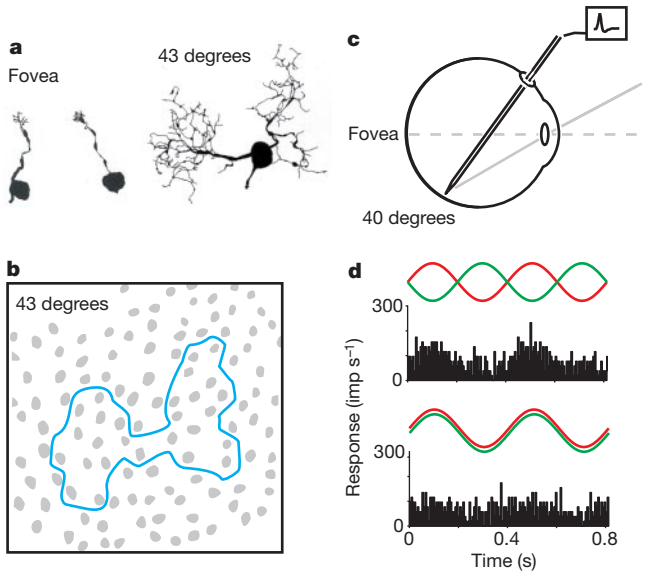

Figure 1 Morphology of PC cells. **a**, Whole-mount view (modified with permission from ref. 9). **b**, Outline of the dendritic field of the peripheral PC cell, which encompasses 27 cones (grey). Sample box 200 × 200 μm. **c**, Diagram of the eye showing the recording configuration. **d**, Peri-stimulus time histograms of a PC cell at 36.5 degrees eccentricity. Responses (impulses sec^{-1}) to red–green isoluminant exchange (top) exceed responses to luminance modulation (bottom).

stimulus, showed a more than 10-fold decrease over this eccentricity range (from 1.073 ± 0.74 at the fovea, to 0.077 ± 0.02 at 30 degrees; Fig. 2a).

Temporal frequency modulation transfer functions were similar in central and peripheral opponent PC cells (Fig. 2b–d): chromatic sensitivity exceeds luminance sensitivity at temporal frequencies below 10 Hz, and is lower than luminance sensitivity for higher temporal frequencies[12,19,20]. Finally, cell responses to red and green LEDs presented at different relative phases and temporal frequencies[16,20] were consistent with selective M or L cone centres for most cells in peripheral retina, although there was slightly greater variability in cone weighting and temporal parameters of peripheral PC cells when compared with their foveal counterparts.

A minority (7/35, 20%) of PC cells in peripheral retina responded weakly, or not at all, to red–green isoluminant modulation. Their centre radii (0.228 ± 0.128 degrees, $n = 5$) were slightly larger than those of opponent PC cells (0.165 ± 0.095 degrees, $n = 16$), but this difference was not significant ($P = 0.24$, t-test). No red–green opponent cells with large, spatially non-opponent ('type 2')[10] receptive fields were encountered. As expected[10,17,18,21], both opponent and non-opponent PC cells had significantly smaller ($P < 0.02$, t-test) receptive field centre radii than phasic, magnocellular pathway cells (0.371 ± 0.145 degrees, $n = 31$). These values are consistent with midget and parasol cell dendritic field radii at the eccentricity range measured[8,9,22].

Non-opponent response characteristics have been reported for midget cells recorded *in vitro* in far peripheral retina, above 50 degrees eccentricity[22], where convergence of cone input is already present at the level of midget bipolar cells. By contrast, at eccentricities below 50 degrees there is little convergence of cone inputs to midget bipolar cells[13], so cone-specific signals are available to PC cell dendrites at these eccentricities. Is the morphology of these PC cells compatible with cone selectivity? A well-known feature of PC cell receptive and dendritic fields in Old World primates is that they are not circular[8,23,24]. Measurement of dendritic field dimensions for a sample of peripheral PC cells gave an average ellipse aspect ratio of

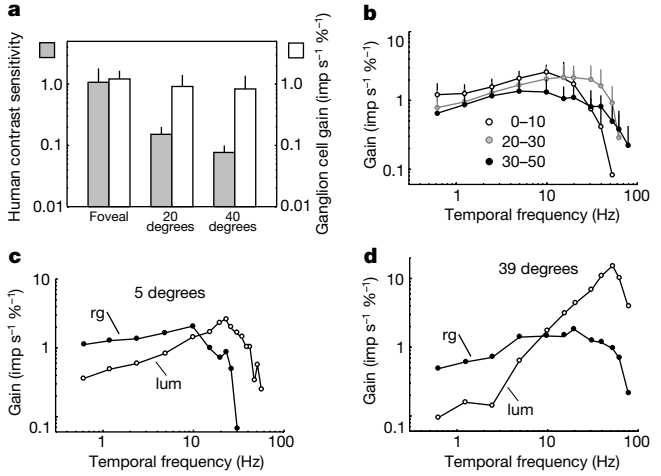

Figure 2 Modulation sensitivity. **a**, Comparison of psychophysical sensitivity of three human observers with opponent PC cell contrast gain to isoluminant red–green modulation. **b**, Temporal modulation transfer functions (tMTF) of opponent PC cells for red–green isoluminant modulation. At least nine cells in each eccentricity range are shown. **c**, **d**, Chromatic (rg) and luminance (lum) tMTFs for sample foveal (**c**) and peripheral (**d**) PC cells show comparable changes in relative sensitivity to the two stimuli with temporal frequency, but the response extends to higher temporal frequencies in the peripheral retina. Error bars in **a** and **b** indicate standard deviations.

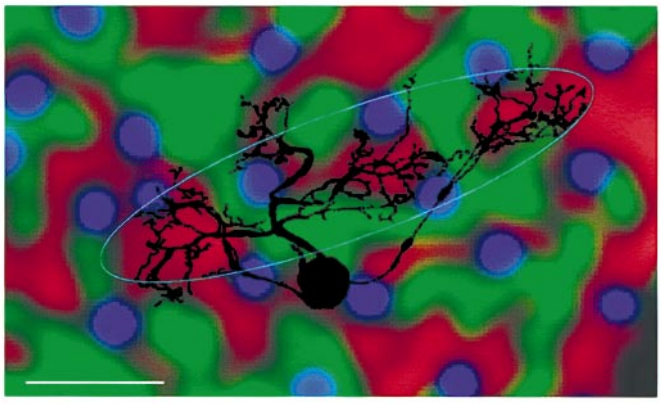

Figure 3 PC cell dendritic tree[9] on a fragment of macaque cone mosaic[25] scaled to local cone density and gaussian filtered. Superposition of ganglion cell dendrites and the L cone mosaic was found by inspection. Local clusters in the dendritic field can be matched to the size of clusters of like (M or L) cones in the mosaic. Equal area ellipse fit to the dendritic field is superimposed. Scale bar, 50 μm.

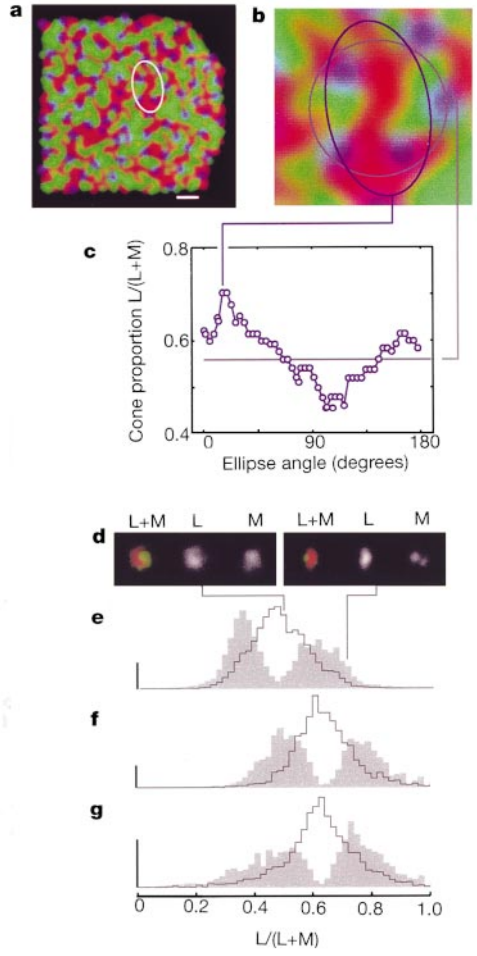

Figure 4 Simulation of cone inputs to peripheral PC cells. **a**, Macaque cone photoreceptor matrix[25], scaled to local cone density (710 cones per mm²)[9] and Gaussian filtered. Scale bar, 0.25 degrees. **b**, Comparison of circular and elliptical sample apertures superimposed on the cone mosaic. **c**, Variation in cone weight with ellipse orientation at this position (points) compared with that for a circular aperture (solid line). Aperture radius 0.13 degrees; ellipse aspect ratio 1.8. **d**, simulated receptive field centres showing combined (coloured) and individual (greyscale) input from M and L cones. Left, circular aperture; right, optimally oriented ellipse from **b**. **e–g**, Distribution of cone weights. Open histograms, distribution for circular apertures; shaded histograms, distribution of optimally oriented ellipses. **e**, Randomized macaque matrix[25]; **f**, macaque matrix[25]; **g**, human subject AN matrix[15]. Vertical scale bar, 200 observations.

1.87. Furthermore, superposition of PC cell dendritic fields with the peripheral cone mosaic (Fig. 3) shows the potential for a high degree of selectivity[8]. We estimated the extent to which the anisotropy in PC cell dendritic fields might influence the balance of cone input, by simulating the connectivity of the peripheral primate retina.

The spatial distribution of cones was taken from the matrices described for the living human and macaque retina[15,25]. We also generated and tested matrices with random M and L cones (Fig. 4a). We compared M and L cone weight obtained from a randomly placed circular sampling aperture with that obtained from an elliptical aperture of variable orientation (Fig. 4b). This showed that even a small circular anisotropy could be the basis of a large change in the ratio of M and L cone input to individual PC cells (Fig. 4c, d).

The ellipse orientation for each simulated cell was optimized to give the greatest segregation of M or L cones. The distribution of cone weight in a large sample of such centres shows a clear bipartite distribution, with a minimum near the average M:L cone ratio, for all the cone mosaics tested (Fig. 4e–g). This is consistent with our physiological finding that most PC cell centres are dominated by either M or L cone input. By contrast, the distribution of circular apertures (or randomly oriented ellipses) shows the expected gaussian form, with a maximum near the average M:L cone ratio for each cone matrix tested (Fig. 4e–g).

The simulations show that dendritic field anisotropy in PC cells might be a sign of cone specificity. The fact that the dendrites of PC cells in human and macaque retina occupy non-overlapping domains[8], which are not preferentially oriented towards the fovea (refs 22, 24; and P.R.M., K. Ghosh, A. Goodchild, unpublished data) is also consistent with this interpretation. The mechanism by which the required match of the dendritic field to clusters of like-type cones would arise is unknown. One possibility is that correlated signals from bipolar cells are a selective stimulus for synapse formation and dendritic growth by PC cells during development. This would lead the dendrites of PC cells to conform to those midget bipolar cells which, in turn, make contact with cones of the same (M or L) type. This idea is supported by evidence that activation of NMDA (*N*-methyl-D-aspartate) receptors leads to dendritic remodelling in ganglion cells[26].

The expected loss of opponent signals in PC cells outside the fovea has been used to argue[6,7] that a non-midget, red–green opponent cell type must underlie the residual colour vision capacity[1,5] of peripheral vision. Our results strike down this objection to considering PC cells as the subcortical origin of the red–green channel for colour vision. □

Methods

Physiology

Adult macaque monkeys ($n = 5$) were anaesthetized and intra-ocular recordings were made using standard techniques[12]. We recorded from a total of 131 cells at eccentricities above 20 degrees: 58 (44%) of these were phasic, magnocellular pathway cells; 54 (41%) were tonic, PC cells; 19 (14%) were tonic, blue-ON cells. We measured antidromic activation latency from the optic chiasm, to ensure that achromatic PC cells could not be mistaken for magnocellular cells[11]. Antidromic latencies fell into three classes: all cells with magnocellular-cell-like properties had latencies close to 5 ms; a second group (PC cells) had latencies of 8–11 ms; and blue-ON cells had latencies around 7 ms. Chromatic sensitivity was measured using luminance-matched LEDs with dominant wavelengths of 639 and 554 nm and time-averaged illuminance close to 2,000 photopic Trolands in maxwellian view[12]. The stimulus subtended 4.7 degrees. Response amplitude is taken as the first Fourier harmonic amplitude at the stimulus frequency. Contrast is expressed as LED modulation relative to maximum. In terms of cone contrast, 100% isoluminant red–green modulation produced 68% Michelson contrast in the M cone and 20% Michelson contrast in the L cone[16]. Receptive field dimensions were measured from responses to drifting sinusoidal luminance gratings[17].

Psychophysics

Three observers (P.R.M., S.G.S. and subject V.B., who did not know the purpose of the experiment) set contrast detection thresholds by the method of adjustment. Stimulus parameters were identical to those for physiological measurements except that the temporal modulation frequency was 1.024 Hz for psychophysics and 1.22 Hz for physiology.

Anatomy

Ganglion cells were filled with Neurobiotin in an *in vitro* preparation of macaque retina[9,22]. The area equivalent ellipse was calculated from a polygon drawn to connect the outermost points of the dendritic field for 98 PC and magnocellular cells. The ellipse aspect ratio for PC cells (1.87 ± 0.64) was significantly greater ($P < 0.01$, *t*-test) than that for magnocellular cells (1.38 ± 0.26).

Modelling

Cone centre position coordinates for macaque M5 (ref. 25) and subject AN (ref. 15) were assigned to a bit-plane image matrix and masked with circular or elliptical apertures. For the L/M random cone matrix the same centre coordinates were used but the identity of each L or M cone was randomly reassigned with equal probability. Aperture dimensions (0.1–0.2 degree radius, 1.5–1.8 aspect ratio) are compatible with measurements of PC-receptive[17,23] and dendritic fields[8,9,22,24] (Fig. 3), and encompass 15–25 cones at 35 degrees. The L and M cones in each aperture were counted using feature-based image detection algorithms (MathWorks, Natick MA, USA). Optimal ellipse orientation was determined using a simple 'hebbian' rule: the dominant (M or L cone) was measured in an initial, circular estimate of the receptive field composition, and then the orientation was chosen that maximized this initial bias. The orientation step size was 22.5 degrees. For illustration purposes, we filtered the cone mosaic (Figs 3 and 4a, b) with a two-dimensional gaussian (radius 0.030 degrees)[27]. Aperture dimensions (radius in degrees and aspect ratio) for histograms were 0.13 and 1.8 (Fig. 4e); and 0.16 and 1.6 (Fig. 4f); 0.16 and 1.6 (Fig. 4g). Cone weight histograms were filtered with 2% uniform noise to reduce artifact from quantization.

Received 20 October 2000; accepted 9 January 2001.

1. Noorlander, C., Koenderink, J. J., Den Ouden, R. J. & Edens, B. W. Sensitivity to spatiotemporal colour contrast in the peripheral visual field. *Vision Res.* **23,** 1–11 (1983).
2. Mullen, K. T. Colour vision as a post-receptoral specialization of the central visual field. *Vision Res.* **31,** 119–130 (1991).
3. Shapley, R. & Perry, V. H. Cat and monkey retinal ganglion cells and their visual functional roles. *Trends Neurosci.* **9,** 229–235 (1986).
4. Lennie, P., Haake, P. W. & Williams, D. R. in *Computational Models of Visual Processing* (eds Landy, M. S. & Movshon, J. A.) 71–82 (MIT Press, Cambridge, MA, 1991).
5. Mullen, K. T. & Kingdom, F. A. A. Losses in peripheral colour sensitivity predicted from "hit and miss" post-receptoral cone connections. *Vision Res.* **36,** 1995–2000 (1996).
6. Calkins, D. J. & Sterling, P. Evidence that circuits for spatial and color vision segregate at the first retinal synapse. *Neuron* **24,** 313–321 (1999).
7. Rodieck, R. W. in *From Pigments to Perception: Advances in Understanding Visual Processes* (eds Valberg, A. & Lee, B. B.) 83–93 (Plenum, London, 1991).
8. Dacey, D. M. The mosaic of midget ganglion cells in the human retina. *J. Neurosci.* **13,** 5334–5355 (1993).
9. Goodchild, A. K., Ghosh, K. K. & Martin, P. R. Comparison of photoreceptor spatial density and ganglion cell morphology in the retina of human, macaque monkey, cat, and the marmoset *Callithrix jacchus*. *J. Comp. Neurol.* **366,** 55–75 (1996).
10. Wiesel, T. N. & Hubel, D. H. Spatial and chromatic interactions in the lateral geniculate body of the rhesus monkey. *J. Neurophysiol.* **29,** 1115–1156 (1966).
11. De Monasterio, F. M. & Gouras, P. Functional properties of ganglion cells of the rhesus monkey retina. *J. Physiol. (Lond.)* **251,** 167–195 (1975).
12. Lee, B. B., Pokorny, J., Smith, V. C., Martin, P. R. & Valberg, A. Luminance and chromatic modulation sensitivity of macaque ganglion cells and human observers. *J. Opt. Soc. Am.* **7,** 2223–2236 (1990).
13. Wässle, H., Grünert, U., Martin, P. R. & Boycott, B. B. Immunocytochemical characterization and spatial distribution of midget bipolar cells in the macaque monkey retina. *Vision Res.* **34,** 561–579 (1994).
14. Packer, O. S., Williams, D. R. & Bensinger, D. G. Photopigment transmittance imaging of the primate photoreceptor mosaic. *J. Neurosci.* **16,** 2251–2260 (1996).
15. Roorda, A. & Williams, D. R. The arrangement of the three cone classes in the living human eye. *Nature* **397,** 520–522 (1999).
16. Smith, V. C., Lee, B. B., Pokorny, J., Martin, P. R. & Valberg, A. Responses of macaque ganglion cells to the relative phase of heterochromatically modulated lights. *J. Physiol. (Lond.)* **458,** 191–221 (1992).
17. Derrington, A. M. & Lennie, P. Spatial and temporal contrast sensitivities of neurones in lateral geniculate nucleus of macaque. *J. Physiol. (Lond.)* **357,** 219–240 (1984).
18. Dreher, B., Fukada, Y. & Rodieck, R. W. Identification, classification and anatomical segregation of cells with X-like and Y-like properties in the lateral geniculate nucleus of Old-World primates. *J. Physiol. (Lond.)* **258,** 433–452 (1976).
19. Gouras, P. & Zrenner, E. Enhancement of luminance flicker by color-opponent mechanisms. *Science* **205,** 587–589 (1979).
20. Lankheet, M. J. M., Lennie, P. & Krauskopf, J. Temporal–chromatic interactions in LGN P-cells. *Visual Neurosci.* **15,** 47–54 (1998).
21. Kaplan, E., Lee, B. B. & Shapley, R. M. in *New Views of Primate Retinal Function* Vol. 9 (eds Osborne, N. & Chader, J.) 273–336 (Pergamon, New York, 1989).
22. Dacey, D. M. Primate retina: cell types, circuits and color opponency. *Prog. Retin. Res.* **18,** 737–763 (1999).
23. Smith, E. L., Chino, Y. M., Ridder, W. H., Kitagawa, K. & Langstom A. Orientation bias of neurons in the lateral geniculate nucleus of macaque monkeys. *Visual Neurosci.* **5,** 525–545 (1990).
24. Watanabe, M. & Rodieck, R. W. Parasol and midget ganglion cells of the primate retina. *J. Comp. Neurol.* **289,** 434–454 (1989).
25. Roorda, A., Metha, A., Lennie, P. & Williams, D. R. Packing arrangement of the three cone classes in primate retina. *Vision Res.* (in the press).
26. Wong, W. T., Faulkner-Jones, B. E., Sanes, J. R. & Wong, R. O. Rapid dendritic remodeling in the developing retina: dependence on neurotransmission and reciprocal regulation by Rac and Rho. *J. Neurosci.* **20,** 5024–5036 (2000).
27. Navarro, R., Artal, P. & Williams, D. R. Modulation transfer of the human eye as a function of retinal eccentricity. *J. Opt. Soc. Am.* **10,** 201–212 (1993).

Acknowledgements

We thank B. Roser and B. Grünert for technical assistance; B. Dreher, U. Grünert, P. Lennie and H. Wässle for helpful discussions and suggestions; A. Goodchild and K. Ghosh for Neurobiotin labelling of ganglion cells; and A. Roorda for cone matrix data.

Correspondence and requests for materials should be addressed to P.M. (e-mail: paulm@physiol.usyd.edu.au).

A CaMK IV responsive RNA element mediates depolarization-induced alternative splicing of ion channels

Jiuyong Xie* **& Douglas L. Black*†**

** Howard Hughes Medical Institute, and † Department of Microbiology & Molecular Genetics, University of California Los Angeles, California 90095-1662, USA*

Calcium regulation of gene expression is critical for the long-lasting activity-dependent changes in cellular electrical properties that underlie important physiological functions such as learning and memory[1]. Cellular electrical properties are diversified through the extensive alternative splicing of ion channel pre-messenger RNAs[2]; however, the regulation of splicing by cell signalling pathways has not been well explored. Here we show that depolarization of GH_3 pituitary cells represses splicing of the STREX exon[3] in BK potassium channel transcripts through the action of Ca^{2+}/calmodulin-dependent protein kinases (CaMKs). Overexpressing constitutively active CaMK IV, but not CaMK I or II, specifically decreases STREX inclusion in the mRNA. This decrease is prevented by mutations in particular RNA repressor sequences. Transferring 54 nucleotides from the 3′ splice site upstream of STREX to a heterologous gene is sufficient to confer CaMK IV repression on an otherwise constitutive exon. These experiments define a CaMK IV-responsive RNA element (CaRRE), which mediates the alternative splicing of ion channel pre-mRNAs. The CaRRE presents a unique molecular target for inducing long-term adaptive changes in cellular electrical properties. It also provides a model system for dissecting the effect of signal transduction pathways on alternative splicing.

BK (Slo) channels participate in the repolarization and fast after-hyperpolarization of action potentials and are important in setting the firing properties of neurons[4,5]. Their diverse properties result largely from extensive alternative splicing of the *Slo* transcript[6–11]. The STREX exon of Slo confers higher Ca^{2+} sensitivity on the channel[3,11–14], and may contribute to the repetitive firing of adrenal chromaffin cells[3,5] and the tuning of hearing frequencies in cochlear hair cells[11,13]. The differential expression of STREX suggests that its splicing is modulated by many physiological factors[3,11,15].

Polymerase chain reaction after reverse transcription (RT–PCR) of Slo mRNA indicated that GH_3 rat pituitary cells include the STREX exon in about 20% of their endogenous Slo transcripts (Fig. 1a, lanes 1, 2, and Fig. 1b). When these cells were depolarized by adding KCl (25 mM), STREX splicing was reduced by 50% in 6 h (lanes 3, 4). Adding the CaMK inhibitor KN93 to the media, before the KCl depolarization, completely blocked this decrease (30 μM, lanes 5, 6). In contrast, the inactive analogue KN92 had only a slight effect (lanes 7, 8). Thus, depolarization of GH_3 cells represses STREX exon splicing, and this repression apparently occurs through a CaMK-dependent pathway.

CaMKs I, II and IV can be activated by cell depolarization and inhibited by KN93. CaMK IV, in particular, is important in depolarization-regulated gene expression[16]. Because all three enzymes are expressed in GH_3 cells (Supplementary Information Fig. 1a), any one of them might be involved in the repression of STREX splicing.

We wanted to determine whether the regulation was acting through the sequences surrounding the STREX exon itself and also was not an effect of transcriptional regulation or RNA degradation. The mouse STREX exon with partial flanking intron sequences

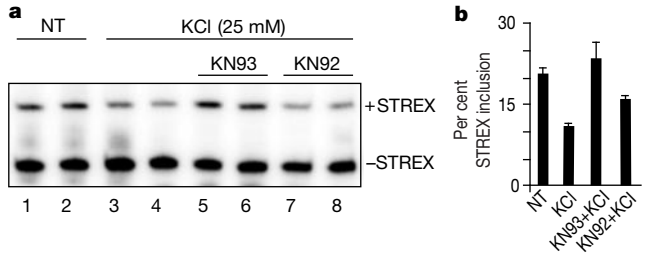

Figure 1 Depolarization-induced changes in STREX splicing depend on CaMK. **a**, Denaturing gel electrophoresis of Slo RT–PCR products from GH_3 cells, including (+) or excluding (–) the STREX exon, 6 h after treatment with nothing (NT, lanes 1 and 2), KCl (lanes 3 and 4), KCl plus KN93 (lanes 5 and 6), or KCl plus KN92 (lanes 7 and 8). Two independent cell samples for each treatment are shown. **b**, Percentage of mRNA containing STREX after the treatments shown in **a**. Results are mean ± s.d., $n = 3$.

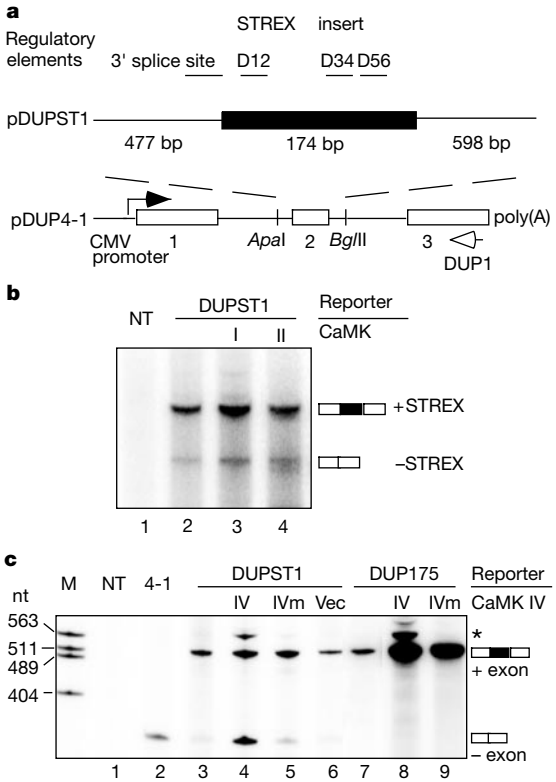

Figure 2 CaMK IV overexpression represses STREX exon inclusion in HEK cells. **a**, The STREX splicing construct pDUPST1. The STREX insert replaces DUP4-1 sequences between the *Apa*I and *Bgl*II sites. The CMV promoter, primer extension primer DUP1 (arrows), exons (boxes), introns (lines) and regulatory elements are indicated. **b**, Primer extension assays of pDUPST1 co-transfected with CaMK I-dCT (I) or CaMK II-dCT (II). **c**, Primer extension assay as in **b** with CaMK IV. M, nucleotide size marker; NT, mock transfection (lane 1); 4-1, pDUP4-1 (lane 2); IV, CaMK IV-dCT (lanes 4 and 8); IVm, CaMK IV-dCTK75E (lanes 5 and 9); Vec, pcDNA3.1(+) (lane 6). Asterisk indicates apparently early terminated products from unspliced mRNA.